Design of Rotating Disc Contactors; Implementation of CFD Tools

Tobias Haderer, Rolf Marr
Department of Chemical Engineering and Environmental Technology
University of Technology Graz
Inffeldgasse 25, A-8010 Graz, Austria

Stefan Martens
Fluent Deutschland GmbH
Birkenweg 14a, D- 64295 Darmstadt, Germany

Matthäus Siebenhofer
VTU-Engineering GmbH
Parkring 18, A-8074 Grambach/Graz, Austria

Key words: Extraction, Rotating Disc Contactor, Computational Fluid Dynamics

Prepared for presentation at the 2004 Annual Meeting, Austin, TX, Nov. 7-12

Copyright © T. Haderer, R. Marr, University of Technology Graz;
S. Martens, Fluent Deutschland;
M. Siebenhofer, VTU-Engineering GmbH

AIChE shall not be responsible for statements or opinions contained in papers or printed in its publications

Abstract

In this project Computational Fluid Dynamics (from Fluent 5.5 up to Fluent 6.1) has been investigated for its accuracy in generating axial dispersion coefficients for the continuous phase in stirred liquid-liquid extraction columns (e. g. Rotating Disc Contactors RDC with 100 mm diameter). As known from literature axial dispersion coefficients determined from single phase flow experiments can be used to estimate two phase flow conditions. By consideration of this fact, only continuous phase flow simulation is mandatory for estimation of reliable data for axial dispersion coefficients. Simulation results show that small changes of the simulated geometry (analyzed number of compartments), injection points and boundary conditions of the inlet and outlet are of rigorous influence for the computed results. The choice of the turbulence models has a significant effect on the simulation results too. To prove simulation and CFD model reliability, simulation results were compared with experimentally obtained data, recorded from several investigations with the test system Toluene/Water and correlations known from literature.

1. Introduction

Information on hydrodynamic parameter such as axial dispersion, hold-up and characteristic velocity is indispensable for the scale-up and design of extraction columns. Many of these design activities must be carried out in laboratories, and plant optimization and determination of chemical and engineering design parameters still need expensive experiments. For reasons of time saving and cost cutting it is desirable to carry out plant and process design with a minimum of scale up steps. Pilot plant tests are expected selectively to confirm design data. Although several correlations have been published for the parameters mentioned above further improvement is necessary because results predicted from CFD simulation strongly depend on the applied correlation and may vary widely [**1**].

The objective of this research work has been to derive design parameters for RDC design with Computational Fluid Dynamics (CFD) and to compare simulation results with experimentally obtained data. The accuracy of current turbulence models and iteration algorithms was investigated and compared with experimental data of Laser Doppler Anemometry (LDA) measurement and CFD calculations carried out previously [**2**]. In addition first experiments were executed to determine Residence-Time-Distributions (RTD) in action-related dependence of operating conditions [**3**]. Although it is not possible to simulate the entire column at present because of the enormous numerical effort and the huge consumption of CPU capacity of CFD codes, it is possible to obtain results of acceptable quality from computation by applying appropriate assumptions such as periodic boundary conditions (translational and rotational) and two-dimensional geometries. The crucial question is, how many and which assumptions need to be made to achieve results that still represent the flow pattern with sufficient accuracy.

2. Apparatus advantages and dimensions of the investigated column

The RDC column is a counter currently operated extractor with the low density dispersed phase (*toluene*) moving from bottom to the top of the column, and the continuous phase (*water*) moving from top to bottom. The major advantages of rotating disc contactors are the simple principle of construction, high throughput and low energy consumption. The agitator consists of a series of rotating, flat discs, which are fixed on the central shaft. Centered between the discs, stator-rings are mounted on the column shell. The stator discs form compartments (space between neighboring stator rings), which limit the effects of axial backmixing.

The choice of a rotating disc contactor for CFD modeling evolved from some basic advantages of the operation principle over several column type extractors. The mesh generation is not as complex as with other column-type extractors such as pulsed columns, Kühni extractors or the asymmetric rotating disc contactors (ARDC). Based on the symmetry of the apparatus the three-dimensional flow pattern can be described in a vertical cutting plane. In cylindrical coordinates the flow parameters only depend on the radius (r) and the height (h) of the column, but not on the angle of rotation (φ) although correctness of the latter assumption had to be proven for the numerical simulation.

Rotation energy is induced by the shear stress of the shaft and the rotor discs. The rate of rotation depends on the physical properties (surface tension, density and viscosity) of both phases, and is in a range of 50 up to 900 rpm. The fluid zone in a compartment consists of two mixing areas (below and above the rotor disc) and a settler zone. The mixing area is located near the rotor disc, where the heavy phase (entering from the compartment above) is mixed with the light phase (entering from the compartment below). In this mixing section high dispersion and also high phase velocity are observed. Because of the energy input and the centrifugal force induced by the rotor the dispersed phase flows radially outward towards the region of the stator rings, where the flow velocity decreases enabling both phases to separate in the settler zone. The light phase moves up and the heavy phase moves down to the next compartment. The phase flux and phase interaction in a compartment is shown in **Figure 1**.

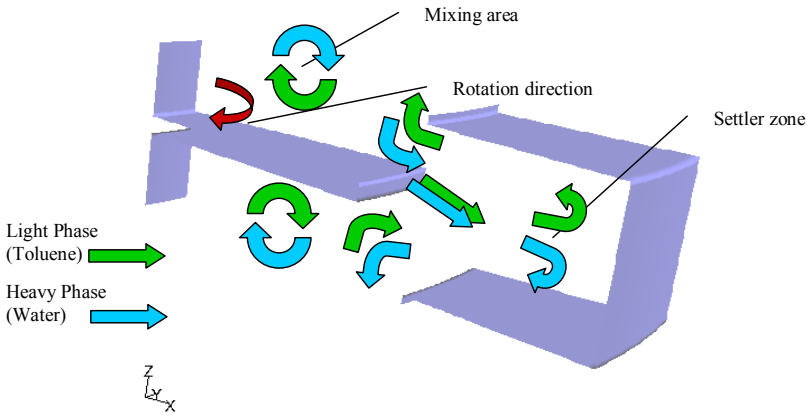

Figure 1: Scheme of phase flux and phase interaction in a RDC-compartment

Residence time distribution (RTD), hold-up and drop size distribution were investigated with an RDC contactor of 100 mm diameter, the construction schematic of which is shown in **Figure 2** (D_{Rotor}=60 mm; D_{Stator}=70 mm; D_{Shaft}=35 mm; H_{Comp}=36 mm) [**4**].

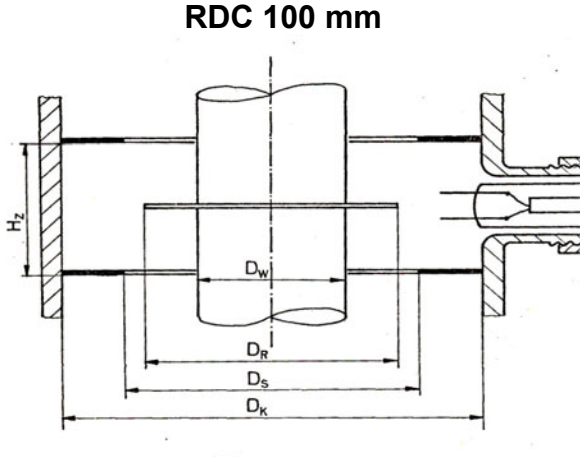

Figure 2: Construction schema of the compartment geometry of the investigated RDC [D_{Rotor}=60 mm; D_{Stator}=70 mm; D_{Shaft}=35 mm; H_{Comp}=36 mm]

3. Development of the Simulation Strategy

In previous research activities [**2**] the influence of the commonly used turbulence models on the results of the calculated flow pattern in RDC extraction columns was discussed. In the present project the realizable k-ε-model and the Reynolds Stress Model were ascertained as models for use. In the continuative work a scale-up parameter (axial dispersion coefficient $E_{ax,c}$) should be computed with the aid of Computational Fluid Dynamics (CFD). For the determination of this parameter the calculation of the residence time distribution (RTD) has to be realized. To compute the RTD of the continuous phase (water) with CFD, a two-phase-flow model (Euler-Lagrange) is needed.

The Euler-Lagrange model provides modeling of spherical particles, bubbles or droplets which are dispersed in the continuous phase. The fluid phase (water) is treated as continuum by solving the time-averaged Navier-Stokes equations, while the dispersed phase is solved by tracking a large number of particles through the previous calculated flow field. Particle tracking is realized by computation of the force balance (equation 1) on each particle moving through the continuum.

$$\frac{dv_P}{dt} = \underbrace{F_W (v_c - v_P)}_{\text{drag force}} + \underbrace{g(\rho_P - \rho_c)/\rho_P}_{\text{gravitation}} + \underbrace{F_i / \rho_P}_{\text{additional forces}} \qquad (1)$$

Because the two-phase approach is only used for the computation of the RTD of the continuous phase it is not necessary to calculate the interaction between the dispersed particles and the continuum. The particles generated for simulation of RTD must have the same physical properties like the continuous phase and they must have a very small diameter of $1*10^{-06}$ m, to ensure that they will strictly follow the flow field [**3, 5**, **6**, **8**].

3.1. Simulation Set-Up

Based on the results of several test computations [**7**], the calculations were carried out by creating a two-dimensional, axis symmetric case file for the simulation. The boundaries of the intake and the outflow face were set periodically, which means that the velocity profile at the inlet is equal to that at the outlet [**2**]. All the flow field calculations were executed with steady state conditions using the segregated, implicit solver with third order interpolation schemes (QUICK [**8**]). Turbulence was considered by implementing the realizable *k*-ε-model. In every simulation the enhanced wall treatment method was used. For the proper implementation of this method the original grid with 0.2x0.2 mm was adapted by computation of the y^+-values in wall adjacent cells shown in **Figure 3**, which should be in the range of 1 to 5. Additionally at least ten cells have to be created within the viscosity-affected near wall region corresponding with $Re_y < 200$ of equation (2), to be able to resolve the mean velocity and turbulent quantities in that region, as demonstrated in **Figure 4**.

$$\mathrm{Re}_y = \frac{\rho y \sqrt{k}}{\mu} \qquad (2)$$

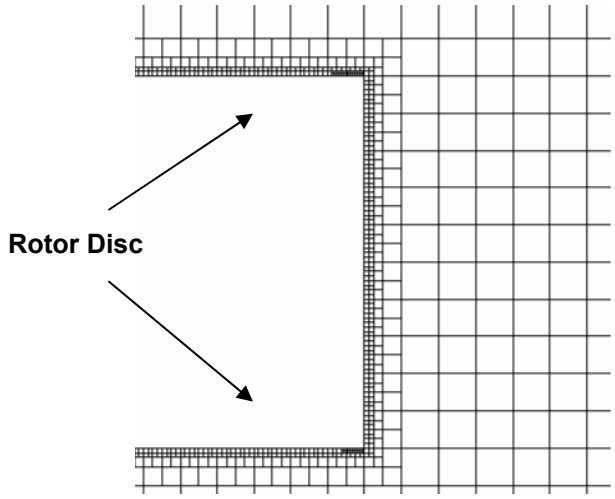

Figure 3: Schematic of the simulation grid

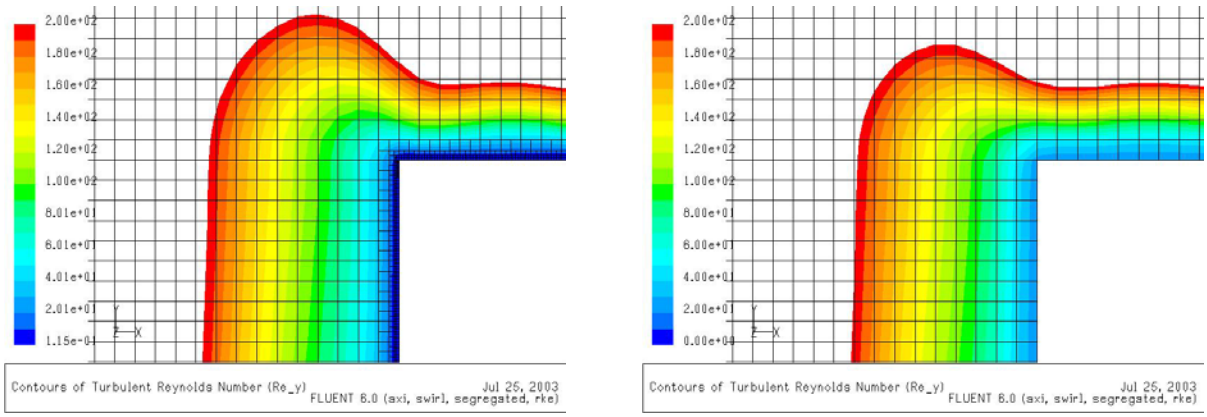

Figure 4: Number of cells in the range of Re_y<200 with and without adaptation [**9**]

3.2. Determination of the Residence Time Distribution

To compute the Residence Time Distribution (RTD) of the continuous phase with the Euler-Lagrange two-phase flow approach injection locations for the particles have to be created. Starting at these injection locations the particle trajectories can be calculated. In this work seven injection locations were generated at which droplets with identical physical properties to the properties of the continuous phase (water) and a droplet diameter of $1*10^{06}$ m were released. As shown in **Figure 5** the injection locations were placed in a plane at the height of a stator-ring with increasing distance of neighboring particles from the stator ring to the shaft). The boundary conditions for the calculation of the particle trajectory at the column shell and the internal equipment were set to reflect and to escape through the inlet plane and the outlet plane, enabling the particles to leave the observation space. The dispersion of particles due to turbulence in the fluid phase was predicted with the stochastic tracking model. The stochastic tracking model includes the effect of instantaneous turbulent velocity fluctuations on the particle trajectories through the use of stochastic methods. In the stochastic tracking panel

each particle trajectory is computed in an auto control mode which finally let to the calculation of as many as 100 to 2000 runs per trajectory in the ongoing project.

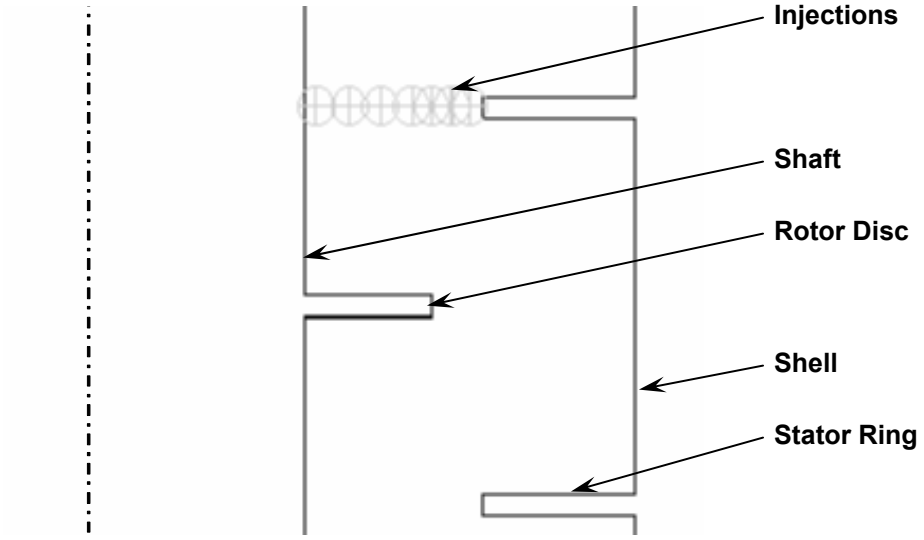

Figure 5: Injection Points at the two dimensional axial symmetric geometry

The particle trajectories were calculated by using the force balance equation on each particle. The transition time was recorded by passing a counting line shown in **Figure 6**. The counting line again was created at the height of a stator ring too. The investigated domain for the RTD is a multiple of the height of a compartment.

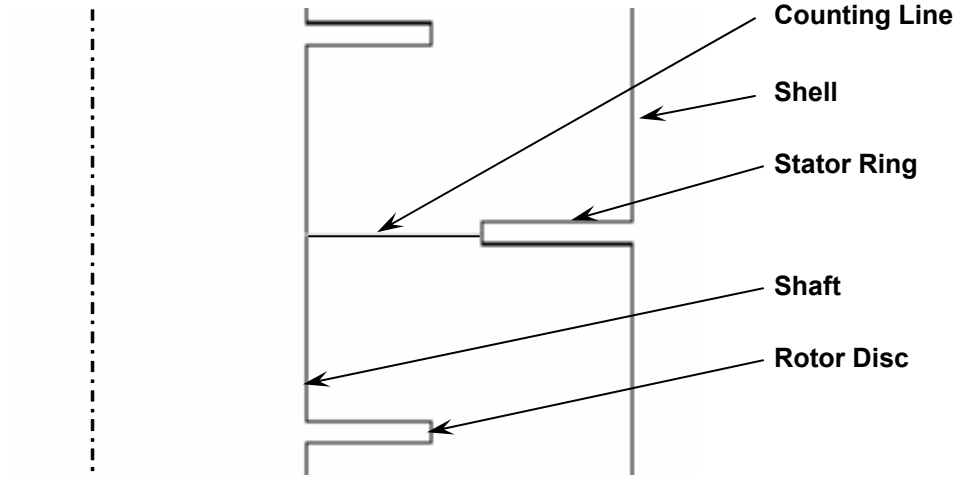

Figure 6: Passing Line at the two dimensional axial symmetric geometry

The transition time was recorded in a "*.dpm-file" which allows the display of a residence time curve. The recorded data were scaled to the maximum number of particles in one time-step and the results were exported to TableCurve®. With TableCurve® the run of the curve was fitted the RTD-solution of Levenspiel [**10**] for the open-open systems dispersion model with the fit parameters Pe-number, the mean residence time τ and the scaling factor A_0.

$$C_0 = A_0 \cdot \frac{1}{2} \cdot \sqrt{\frac{\tau \cdot \mathrm{Pe}}{\pi \cdot t}} \cdot \exp\left[\frac{-\tau \cdot \mathrm{Pe} \cdot \left(\frac{1-t}{\tau} \right)^2}{4 \cdot t} \right] \tag{3}$$

Because of data normalization a scaling factor (A_0) was implemented into equation (3) to ensure equal area of the simulated and the fitted curves (**Figure 7**).

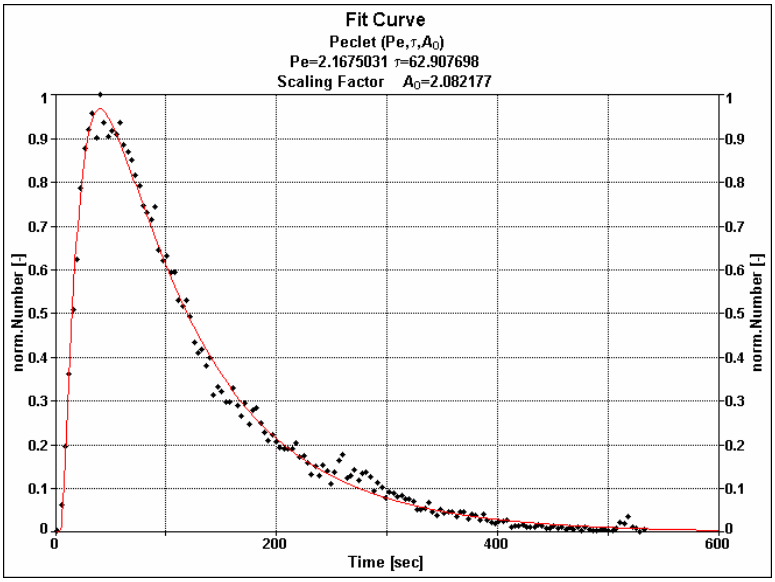

Figure 7: Fit curve (full line) and fit parameters computed with TableCurve®

With the computed Pe-number and mean residence time τ the dispersion coefficient $E_{ax,c}$ and the mean flow velocity v_c were determined according to:

$$E_{ax,c} = \frac{v_c \cdot L}{\mathrm{Pe}} \tag{4}$$

$$v_c = \frac{L}{\tau} \tag{5}$$

The results generated through CFD simulation were compared with experimental data and empirically determined correlations (Bauer [**11**] (equation (6); Kumar and Hartland [**12**] (equation (7)) to finally establish a simulation set-up with satisfying accordance of the simulated and the real flow field.

$$\frac{E_{ax,c}}{\bar{v}_c \cdot L} = k_1 + k_2 \cdot \left(\frac{N \cdot D_R}{v_c} \right)^{m_1} f(G) \tag{6}$$

$$\frac{1}{\mathrm{Pe}_c} = \frac{E_{ax,c}}{\bar{v}_c \cdot L} = K + \left(\frac{\mathrm{Re}_n^{0,83}}{\mathrm{Re}_c} \right) f(G) \tag{7}$$

4. Results

In first simulation runs, the flow field of four compartments was calculated for different operating conditions without disperse phase flow by varying the flow rate of the continuous phase from 28.3 l/h to 160 l/h and the rate of rotation from 0 rpm to 900 rpm. The flow pattern was calculated considering turbulence with the realizable k-ε model [**2**]. The Residence Time Distribution (RTD) of the continuous phase was estimated for two compartments in the center. The first and the last compartment were reserved for inlet and outlet. **Figure 8** shows the comparison of the calculated RTD data with data records from experiments executed in the RDC extractor of 100 mm diameter.

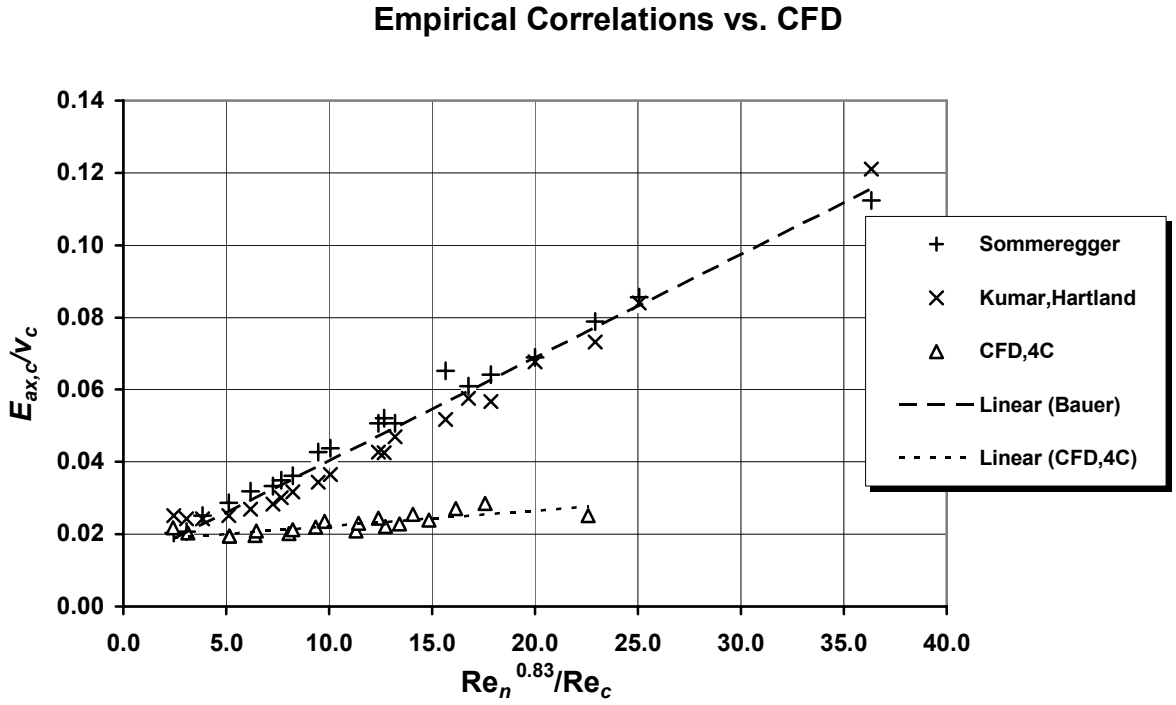

Figure 8: Comparison of experimental data for $E_{ax,c}/v_c$ with empirical correlations and CFD data [**3**]

The generated results clearly show that at low rate of rotation and high continuous phase throughput only simulation results match experiments with acceptable accordance. The simulated mean velocity deviated from experimental data tremendously. The simulated mean velocity data were larger than the experimentally obtained values. As a consequence the data-points of the CFD,4C-line in **Figure 8** do not match the data from experiments. The discrepancy between CFD simulation and experiments at higher rate of rotation is significant. Nevertheless it was demonstrated that CFD is able to achieve acceptable results for low rate of rotation and moderate to high throughput of the continuous phase.

Strategy of improvement of CFD-results focused on extension of the simulation area (number of compartments), variation of disperse phase boundary conditions and application of different turbulence models.

Improvement of CFD simulation depended very much on the improvement of the simulation software. The software versions Fluent 5.5 up to Fluent 6.0 were limited to application of two parameter turbulence models in combination with the Discrete Phase Model (DPM). The latest software version of Fluent (Fluent 6.1, released 2004) enables calculation of the RTD with implementation of the Reynolds Stress turbulence model.

4.1. Influence of the Inlet Boundary Conditions

To analyze the influence of the geometry size a simulation series was worked out with a simulation area of 8 compartments (CFD,8C). The residence time distribution calculations of the continuous phase were extended to 4 compartments. Two compartments below the passing line and two compartments above the injection plane were left for consideration of recirculation zones. Additionally the preliminary simulations showed that many particles are lost at the inlet face by simulation of a too small area.

Limiting the simulation area to the inlet causes an irrecoverable loss of particles for RTD simulation. These “late” particles will pass the counting line retarded to injection and affect the RTD graph by a significant tailing as shown by the comparison of data dots from simulation and the experimentally determined RTD curve in **Figure 9**. Additionally the loss of particles creates a smaller mean residence time (τ) compared with experiments. . To avoid the significant effect of tailing on the axial dispersion coefficient the boundary condition for the disperse phase was set on reflect as a first approximation for the inlet plane.

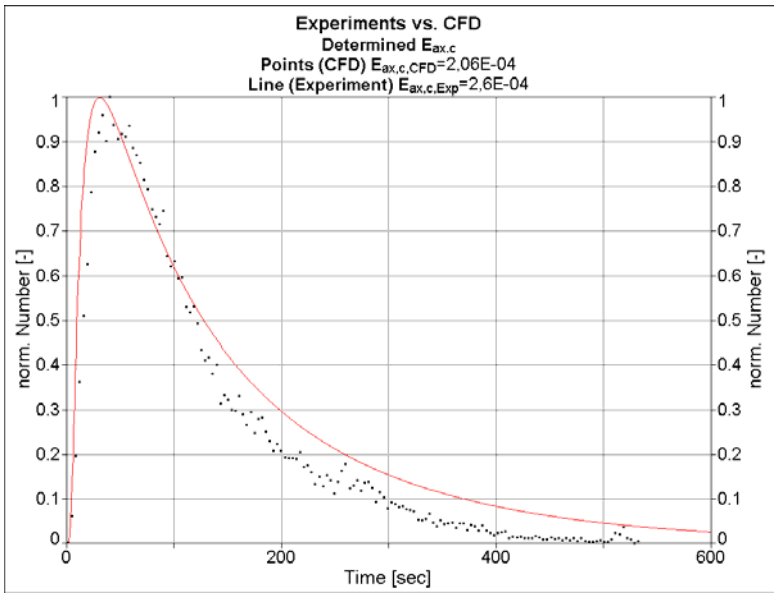

Figure 9: Comparison of CFD data with experiments (full line = Experiments and points = CFD data) [**9**]

In addition the simulated mean velocity, which deviates slightly from experiments only, was adjusted to the experimental data to obtain conformity of the x-axis data and consequently better comparability of simulated axial dispersion coefficient. The new computed data are herein after referred to as CFD,4C,opt and CFD,8C,opt in **Figure 10** Therefore only the Pe-number and the scaling factor (A_0) were left for variation in the fit function (equation (3)).

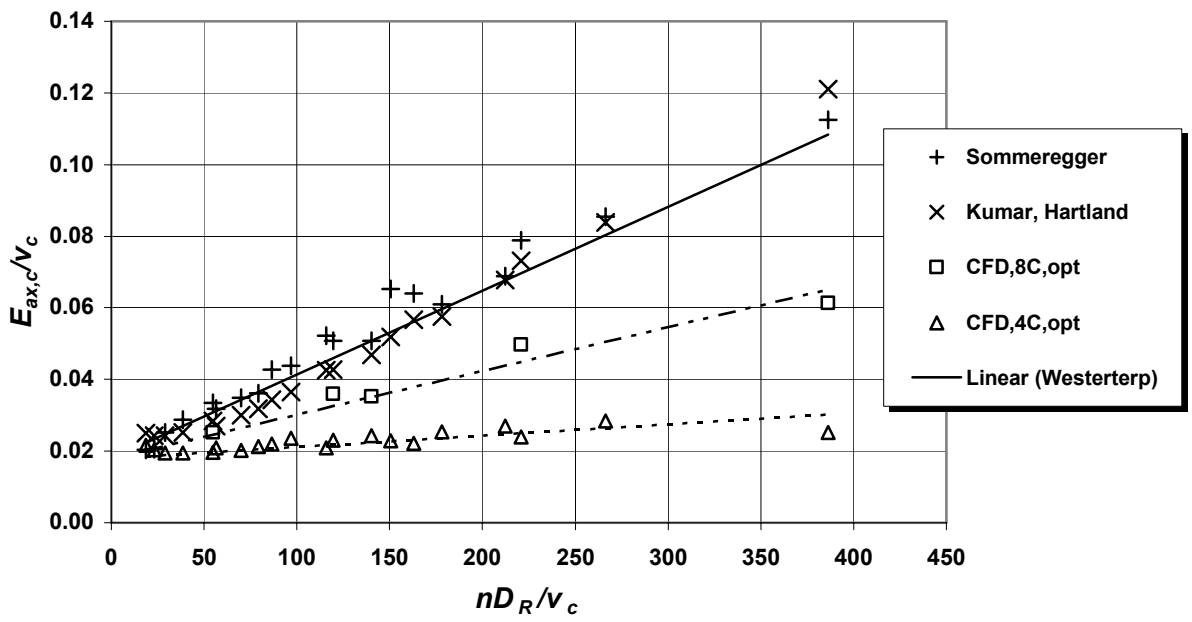

Figure 10: Comparison of optimized CFD data with empirical correlations and experiments

4.2. Influence of the Number of Compartments

As shown in **Figure 10** the enlargement of the simulated geometry improves the results at higher energy input and lower throughput but still does not result in satisfying accordance of experiments and simulation.

From the comparison of the 8 compartments simulation results with the 4 compartments simulation runs it can be concluded that further enlargement of the simulation area may (and seem to) improve the simulation results. Therefore the RTD simulation was carried out for 16 compartments. Simulation was performed for a representative mean operation state. The volumetric throughput of the continuous phase was set to 160 l/h and the rate of rotation was set to 900 rpm. To ensure comparability the flow pattern of the 16 compartments file was compared with the 4 compartments calculations. The comparison is shown in **Figure 11**.

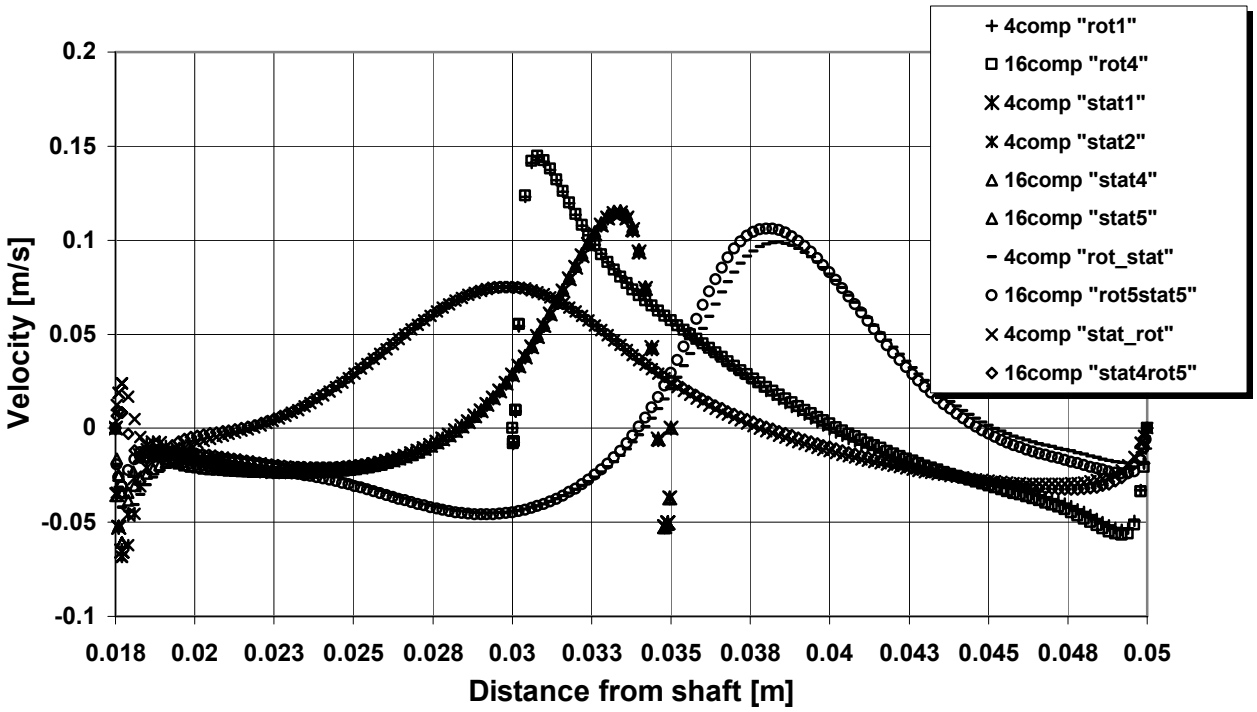

Figure 11: Calculated axial velocities at different heights in a compartment;
Parameter: number of compartments

With the results displayed in **Figure 11** good accordance between the calculated flow patterns is ascertained. Close to the rotor shaft deviation can be detected. These deviations are induced by the energy input of the mixer and the stochastic turbulence modeling which establishes wakes moving along the mixer wall [**13**].

In this simulation runs the disperse phase boundary condition reflect at the inlet was compared with escape again. The flow field of 16 compartments was calculated and the residence time distribution of 4, 6, 8 and 10 compartments was determined. The DPM calculations were always carried out for the compartments in the center of the geometry which resulted in run times of approximately five days. The results are shown in **Figure 12**.

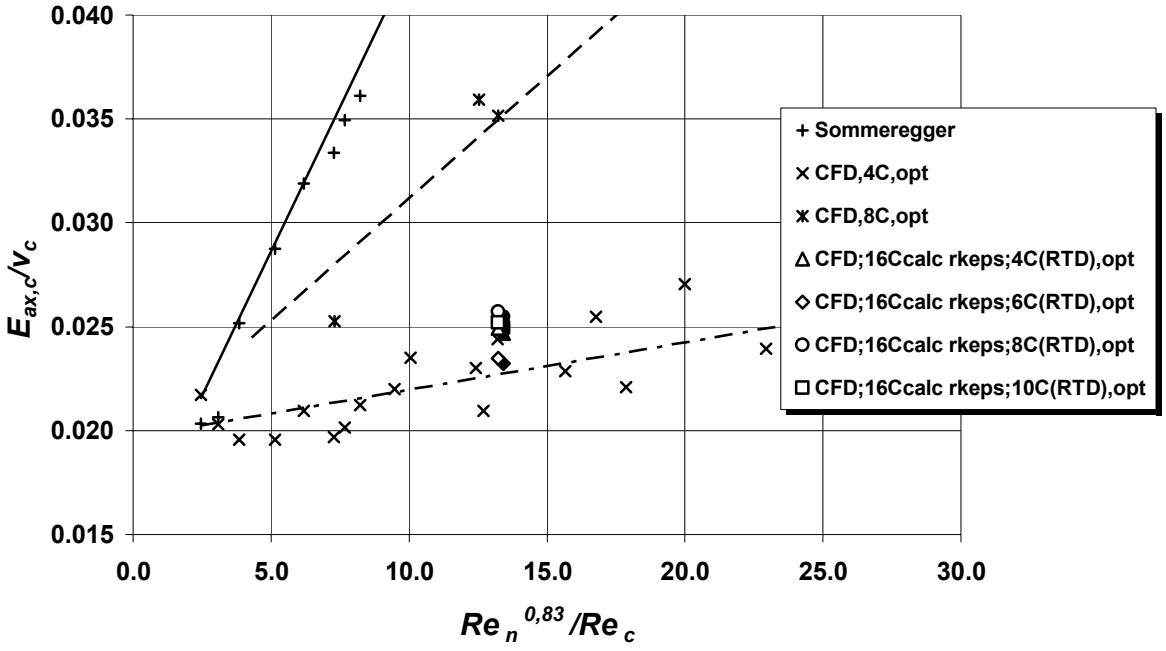

Figure 12: Comparison of axial dispersion coefficients (operating conditions: 160 l/h; 900 rpm; turbulence model: realizable *k*-ε model)

As demonstrated with the series of "16 compartments" (CFD;16Ccalc) simulations in **Figure 12** the expected improvement of the simulated dispersion coefficient through enlarging the simulation area was definitely not observed. As a consequence RTD is not influenced by the number of the compartments used for the DPM calculations. The improvements of simulated RTD in comparison of the 4 compartments simulation runs and the 8 compartments simulation runs only depend on the boundary conditions. The 16 compartments simulations result in comparable axial dispersion coefficients. No dependency of the calculated results on the employed inlet boundary conditions (reflect or escape) for the disperse phase can be ascertained. Enlargement of the simulation area has a minor effect on the quality of simulation.

4.3. The Reynolds Stress Model (RSM)

Based on poor accordance of CFD calculation with experiments, the DPM research was retried using the Reynolds Stress model (RSM). Simulation of flow pattern with RSM differs significantly from simulation with the realizable *k*-ε model [**2**]. Comparison of the models shows, that at high rate of rotation the RS Model produces a much stronger effect of the energy input on the flow pattern in radial direction Therefore the RTD investigations were performed again with implementation of the Reynolds Stress Model. To retain a better survey the calculations were executed at same operating conditions (RSM; 160 l/h; 900 rpm; 16 compartments) as applied in the simulations with the realizable k-ε model. The inlet boundary condition for the disperse phase was set on "trap", which stops the trajectory calculation for

lost particles. With this boundary condition the number of particles is identified which quits simulation area at the inlet. In this case the simulated flow fields are not equal and a comparison of the velocities is nonsensical. The DPM iteration was carried out for 2, 6 and 10 compartments. The results are displayed in **Figure 13**. In these simulations the mean velocity of simulations was in good agreement with experiments and no unification procedure was necessary.

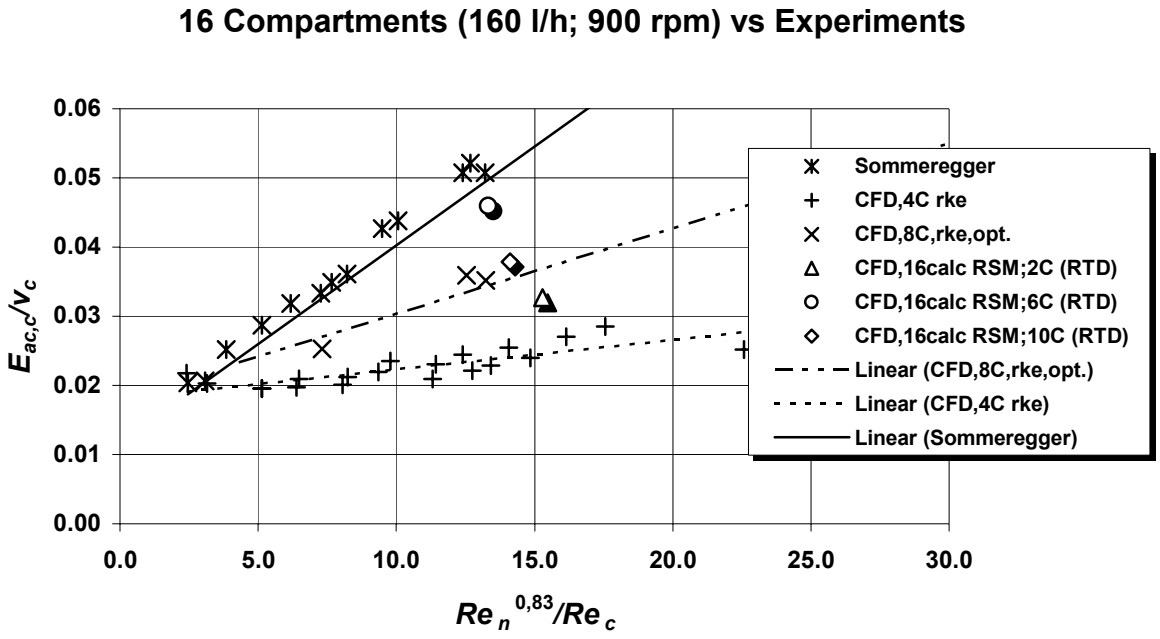

Figure 13: Comparison of axial dispersion coefficients (160 l/h; 900 rpm; RSM)

As can be figured out from **Figure 13** the calculated axial dispersion coefficients ($E_{ax,c}$) diverge. The results displayed in **Figure 13** differ tremendously from the results illustrated in **Figure 12**. When using the Reynolds Stress turbulence model for simulation a significant influence of the number of compartments is shown. Best accordance of simulation results with experiments and empirical correlations was obtained with the 6 compartments RTD model. For 2 compartments the residence time curve has a very narrow distribution (**Figure 14**) wherefore the results of the fit procedure are not very well defined. The result of the 10 compartments computation as well indicates simulation conditions beyond (outside) the optimum range. The reason for this unexpected tendency originates in the loss of particles. Not only trapped particles at the inlet also particles which are leaving the column at the outlet are lost in RTD calculations. These particles influence the shape of the curve at extended residence time and as a consequence the axial dispersion coefficient (**Figure 9**). This effect will be enforced by enlarging the RTD computation area and maintaining calculation geometry of the flow pattern.

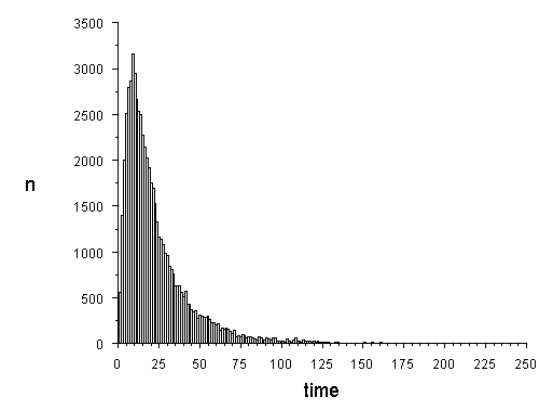

Figure 14: Histogram of the 2 Compartments RTD calculation (160 l/h; 900 rpm; RSM)

In a next step worst case simulation conditions (56.3 l/h throughput and 900 rpm) was investigated with the same simulation parameter settings as listed above. Again 2 and 6 compartments files were created and the RTD was determined in a simulation geometry of 16 compartments. The residence time curves are shown in **Figure 15** and **Figure 16**.

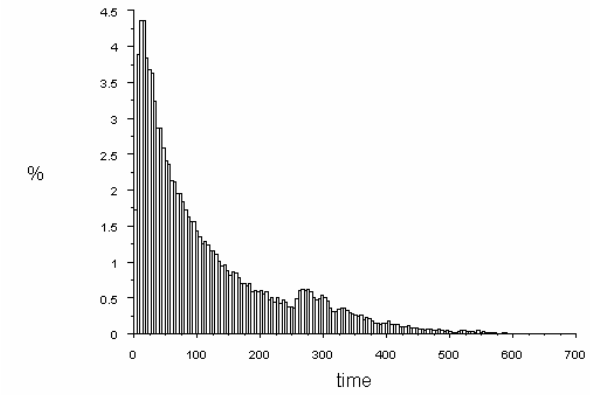

Figure 15: Histogram of the 2 Compartments RTD calculation (56.3 l/h; 900 rpm; RSM)

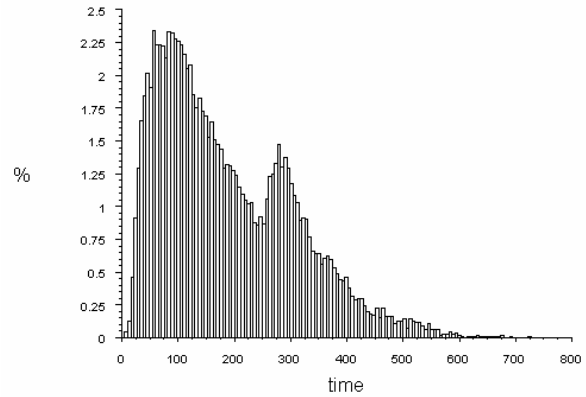

Figure 16: Histogram of the 6 Compartments RTD calculation (56.3 l/h; 900 rpm; RSM)

In **Figure 15** and **Figure 16** the residence curves show surprising result. A second (at 250-300 seconds) and even a third peak (circa 500 seconds) are displayed. The peaks are much more distinct in the 6 compartments simulation in **Figure 16** and do not permit further

computations. An explanation could be the loss of particles. As already mentioned above the trapped boundary condition is implemented to count particles which are leaving the computation area at the inlet. In the 2 compartments simulation 204 particles and in the 6 compartments simulation 594 particles were captured at the inlet face. At least the same number of particles is missed in the parameter determination (axial dispersion coefficient and mean residence time). The relative error is shown in **Figure 17**.

2 compartments RTD calculation		6 compartments RTD calculation	
Particles		Particles	
tracked	10500	tracked	10500
counted	166000	counted	152000
aborted	54	aborted	58
trapped	204	trapped	594
escaped	10242	escaped	9848
missing	408	missing	1188
mean crossing	16	mean crossing	16
% error	4%	% error	12%

Figure 17: Particle tracking (16 Compartments, 56.3 l/h; 900 rpm; RSM)

The 2 compartments simulation results were used for computing the axial dispersion coefficient. In addition the computation area was enlarged again (simulation area of 32 compartments) to reduce the effect of particle loss. With the 32 compartments file RTD calculations for 4 compartments were executed (CFD,32calc). The results of these calculations are shown in **Figure 18**.

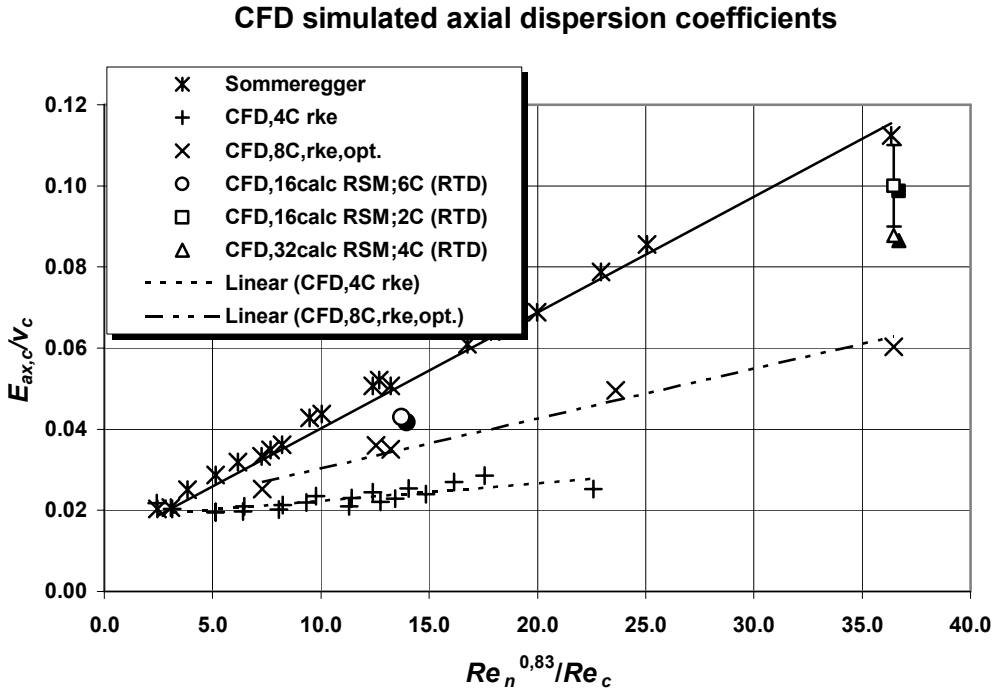

Figure 18: Axial dispersion coefficients determined with different CFD settings

Figure 18 shows that the calculations executed with the Reynolds Stress turbulence model are in better accordance with experiments and empirical correlations. Comparison of 32 compartments with 16 compartments results in a deviation of about 10 %. For comparison the mean deviation of empirical correlations from experiments is in the range of 20% [**12**].

5. Summary

Target of investigations was to establish simulation of axial dispersion coefficients for the continuous phase in RDC extraction columns. After optimization of the parameter settings the computed data are in sufficient accordance with experimental data and empirical correlations. It was shown that the selection of the turbulence model is of predominating influence. As displayed in the results the RS-model proved best in modeling the rotating disc contactor extraction column. The influence of the computation area on RTD was worked out too. The results of RSM simulations lead to the conclusion that RTD investigation must be executed in large simulation geometries. It has to be ensured that particle leaving the computation area against the main flow direction can be kept at minimum. Application of trapping boundary conditions is therefore recommended.

6. References

1 Moris, M. A.; Diez, F. V.: Coca, J.: Hydrodynamics of a rotating disc contactor, Sep. and Purif. Tech. 11, 79-92, 1997

2 Haderer, T.; Huber, Ch.; Marr, R.; Martens, S.: Numeric flow simulation of a RDC extraction column; Proceeding of 15th International Congress of Chemical and Process Engineering, CHISA 2002, (CD-ROM 1295.pdf); Praha, CZE, 25.-29.8.2002

3 Haderer, T.; Marr, R.; Martens, S.; Siebenhofer, M.: Apparatus Design in Liquid-Liquid Extraction; CFD Supported Modelling of Residence Time and Residence Time Distribution, Proceedings of AIChE Annual Meeting 2003, San Francisco, CA, Nov 16-21, 2003; OMNIPRESS American Institute of Chemical Engineers, New York, NY, 2003; 314c.pdf, 2003

4 Sommeregger, E. Hydrodynamik in Drehscheibenextraktoren; PhD Thesis; Institut für Thermische Verfahrenstechnik und Umwelttechnik, TU Graz, 1980

5 Kolb, P.; Bart, H.-J.; Fischer, L.: Entwicklung einer Miniplant-Extraktionskolonne; Chemie Ingenieur Technik, 74, 3, 243-247, 2002

6 Mehrle, Y.: Strömungssimulation einer gerührten Extraktionskolonne zur Bestimmung hydrodynamischer Kenngrößen, Master Thesis, Universität Kaiserslautern, 2002

7 Huber, C.: Numerische Simulation der Strömungszustände in einer RDC Extraktionskolonne, Master Thesis, TU Graz, 2002

8 Fluent User Guide, 2001

9 Kurz, Ch.: Numerische Strömungssimulation einer RDC-Extraktionskolonne und Evaluierung der Ergebnisse, Master Thesis, TU Graz, 2003

10 Levenspiel, O.: Chemical Reaction Engineering, John Wiley & Sons, New York, 1962

11 Bauer, R.: Die Längsvermischung beider Phasen in einer gerührten Extraktionskolonne, Dissertation ETH Zürich, 1976

12 Kumar, A.; Hartland, S.: Prediction of Axial Mixing Coefficients in Rotating Disc and Asymmetric Disc Extraction Columns; Can. J. Chem. Eng.; 77-89; 1992

13 Haderer, T.: Numerische Simulation einer RDC Extraktionskolonne zur Bestimmung hydrodynamischer Kenngrößen; PhD Thesis; TU Graz, 2004